

# Mechanosensitive transient receptor potential vanilloid type 1 channels contribute to vascular remodeling of rat fistula veins

Yih-Sharnng Chen, MD, PhD,<sup>a</sup> Ming-Jen Lu, MD,<sup>b</sup> Ho-Shiang Huang, MD, PhD,<sup>c</sup> and Ming-Chieh Ma, PhD,<sup>d</sup> *Taipei and Hsinchuang, Taiwan*

**Objective:** We previously showed that matrix metalloproteinases (MMPs) contribute to tremendous blood flow-induced venous wall thickening during the maturation of an arteriovenous fistula (AVF). However, how veins in the fistula sense a dramatic change in the blood flow remains unknown. Because mechanosensitive transient receptor potential vanilloid channels (TRPVs) are present in the endothelium, we examined whether the Ca<sup>2+</sup>-permeable TRPVs play a role in remodeling of fistula veins.

**Methods:** The fistula veins were generated at femoral AVF of Wistar rats. Changes in the hemodynamics and the width and internal radius of the iliac vein were studied at 3, 7, 14, and 28 days, then the iliac vein was removed and examined for changes in wall thickness and protein or mRNA expression by immunofluorescent stain, Western blot, or real time PCR. Changes in MMP2 activity was examined by gelatin zymography. Two ligatures were performed in iliac vein to prevent venodilatation to confirm the effect of dramatic changes in hemodynamics on TRPV expression. The specific role of TRPV was studied in another group of fistula veins given with capsaizepine via a subcutaneous mini-osmotic pump for 28 days.

**Results:** The fistula veins demonstrated high flow/wall shear stress (WSS), wall thickening, and venodilatation compared with control veins. The WSS increase was positively correlated with upregulation of TRPV1, but not TRPV4. Narrowing fistula veins prevented TRPV1 upregulation, indicating that high flow directly upregulates TRPV1. We examined the underlying signaling components and found that enhanced Ca<sup>2+</sup>/calmodulin-dependent protein kinase II (CaMK II) activity upregulated endothelial nitric oxide synthase (eNOS) and downregulated arginase I in the fistula veins. These changes were reversed by a CaMK II inhibitor. The relative levels of eNOS and arginase I activity consequently augmented NO formation, which coincided with an increase in MMP2 activity. Chronic inhibition of TRPV1 in the fistula veins by capsaizepine showed no effect on high flow and TRPV1 expression, but markedly attenuated WSS, which was concomitantly associated with attenuation of CaMK II activity, NO-dependent MMP2 activation, and remodeling.

**Conclusion:** These findings indicate that TRPV1 is essential in the remodeling of AVFs and that WSS leads to TRPV1 upregulation, which then enhances remodeling, therefore, inhibition of TRPV1 pathway may prolong the lifespan of an AVF by decreasing WSS and vein wall remodeling. (*J Vasc Surg* 2010;52:1310-20.)

**Clinical Relevance:** This study reveals that enhanced endothelial mechanosensation is requisite for the fistula remodeling in response to dramatic hemodynamic changes. Moreover, our findings demonstrate that Ca<sup>2+</sup> signal triggered by TRPV1 upregulates eNOS and downregulates arginase I and which enhances NO formation to lead to MMP2 activation in extracellular matrix remodeling of fistula veins. These findings enhance understanding of the basic biologic mechanisms in the venous remodeling. The need for TRPV1-mediated remodeling suggests that clinical strategies to blunt mechanosensation of fistula veins during maturation might be more successful or prolong the life span of fistula veins if TRPV1 are inhibited as a part of the surgical or follow-up treatment.

An arteriovenous fistula (AVF) is the preferred vascular access for patients with end-stage renal disease requiring

From the Department of Cardiovascular Surgery, National Taiwan University Hospital, Taipei,<sup>a</sup> Department of Surgery, Shin Kong Wu Ho-Su Memorial Hospital, Taipei,<sup>b</sup> Department of Urology, National Taiwan University Hospital, Taipei,<sup>c</sup> and School of Medicine, Fu Jen Catholic University, Hsinchuang.<sup>d</sup>

This work was funded by the Shin Kong Wu Ho-Su Memorial Hospital to M.C.M. and M.J.L. (SKH-FJU-96-06, 97-14), and National Science Council of the Republic of China to Y.S.C., H.S.H. and M.C.M. (97-2314-B-002-046-MY3 and 98-2314-B-030-004-MY3).

Competition of interest: none.

Reprint requests: Ming-Chieh Ma, PhD, Fu Jen Catholic University School of Medicine, 510 Chungcheng Rd, Hsinchuang 242, Taipei, Taiwan (e-mail: med0041@mail.fju.edu.tw).

The editors and reviewers of this article have no relevant financial relationships to disclose per the JVS policy that requires reviewers to decline review of any manuscript for which they may have a competition of interest.

0741-5214/\$36.00

Copyright © 2010 by the Society for Vascular Surgery.

doi:10.1016/j.jvs.2010.05.095

hemodialysis.<sup>1</sup> Following surgical creation, fistula veins are immediately challenged with a tremendous blood flow and high wall shear stress (WSS), and the lumen gradually dilates to reduce WSS.<sup>1,2</sup> Growth of new cells and formation new matrix in the venous wall results in wall thickening of intima or media while greatly increasing the risk of AVF failure.<sup>2,3</sup> Therefore, strategies that can optimize remodeling of the fistula veins but without affecting venodilation and hemodynamic changes are needed to prolong the useful lifespan of the AVF. We showed previously that a rat AVF created at the femoral artery and vein shares features similar to clinically generated AVF constructed for hemodialysis, ie, high blood flow and low pressure are seen in the fistula veins, and changes in the collagen deposition and tissue expression of matrix metalloproteinases (MMPs) and tissue inhibitor of metalloproteinases are responsible for venous remodeling.<sup>4</sup> However, how the increased blood flow is detected by the fistula vein to induce vascular remodeling by MMPs is unknown.

The endothelium is an important interface in converting the physical force of blood flow or WSS to biochemical signaling, which controls the plasticity of the underlying smooth muscle cells (SMCs).<sup>5</sup> Among various cellular signals,  $Ca^{2+}$ -dependent mechanotransduction for releasing vasoactive substances such as nitric oxide (NO) plays an important role in the regulation of tissue perfusion.<sup>6</sup> Impairment in sensing the flow-generated WSS attenuates vasodilatation and is recognized as a hallmark of endothelial dysfunction in various presentations of cardiovascular diseases.<sup>7</sup> In the dog AVF, chronic increases in blood flow enhance the response of endothelium- and NO-dependent vasodilatation to acetylcholine and  $\alpha 2$ -adrenergic stimulation in fistula veins.<sup>8</sup> Moreover, studies in rats showed that chronic increases in blood flow in the aorta and in the mesenteric artery, caused by an aortocaval fistula and aortic ligation, respectively, enhanced expression of endothelial NO synthase (eNOS), whereas reduction of blood flow decreased eNOS expression.<sup>9,10</sup> These observations indicate that NO generated by enhanced eNOS function is important for fistula vessels in their adaptation to increased blood flow. However, how fistula vessels adapt increased blood flow well by enhanced eNOS function and NO generation is unclear.

Different members of the transient receptor potential channel (TRP) family have been identified in the endothelium.<sup>7</sup> Of particular interest in mechanotransduction are the TRP vanilloid (TRPV) subfamily because both TRPV1 and TRPV4 play a role in regulation of vascular tone.<sup>7,11,12</sup> The presence of TRPV4 in the endothelium of the rat carotid artery is a response to increased WSS and causes endothelium-dependent vasodilatation.<sup>12</sup> TRPV1 not only functions as an endothelial vasorelaxant, but also acts as a mechanoreceptor or mechanotransducer in the renal pelvis, bladder, and carotid sinus in response to elevation of the intraluminal hydrostatic pressure.<sup>13-15</sup> Moreover, a few studies have detected functional TRPVs in fistula veins. These observations led us to formulate the hypothesis that TRPV present in the venous endothelium may act as a mechanosensor to detect the increases in flow/WSS after AVF creation. NO plays a key role in the control of MMP activity in flow-induced remodeling.<sup>16</sup> We therefore assessed whether NO-dependent MMP stimulation is regulated by TRPVs in vascular remodeling of the fistula vein.

## METHODS

**AVF creation in rats.** The experimental protocols used 200 to 220 g female Wistar rats (Laboratory Animal Center, National Taiwan University, Taipei, Taiwan) and were approved by the Institutional Animal Care and Use Committee. The arteriovenous anastomosis at the left femoral artery and vein (Fig 1, A) was created as described previously.<sup>4</sup> Briefly, the fistula veins were generated by invagination of distal end of the left femoral artery into the femoral vein after venotomy. A ligature between the two vessels using 8-0 silk is enough to prevent the artery from detaching after reflow. In the control veins, the left femoral artery was cut, but invagination was not performed. Tem-

poral changes in hemodynamics and vein thickness were examined 0, 3, 7, 14, or 28 days postoperatively.

**Hemodynamic measurements.** On the experiment day, animals were anesthetized with intraperitoneal pentobarbital sodium (50 mg  $kg^{-1}$ ). After a midline laparotomy was performed to expose the lower abdominal vessels, the external width (mm) of the left iliac vein was determined from photographs taken with a calibrated scale. The iliac vein (2 cm cephalad of the fistula) was then isolated from the surrounding tissue to measure the blood flow ( $Q$ , mL  $min^{-1}$ ) using a flowmeter (Transonic, Ithaca, NY). The pressure in the veins was measured by direct puncture with a 30-gauge needle connected to polyethylene tubing (PE-10) and a pressure transducer.<sup>4</sup> After cutting a 2-mm segment of iliac vein and opening it, the length of venous strip, ie, the circumference, was determined from photographs taken with a calibrated scale. The internal diameter (mm) was calculated by dividing the circumference by  $\pi$ . WSS was estimated using  $\tau = 4\eta Q/\pi r^3$ , where  $\eta$  and  $r$  are the blood viscosity (0.035 poise) and the internal radius,<sup>17</sup> respectively. Six rats were studied at each time point and none showed complications such as intravascular coagulation or stenosis. Then the venous strip was prepared for histological examination and biochemical assays. Because there was no difference in the control veins obtained at different time-points, we pooled those samples.

**Restriction of blood flow.** In the separate groups, two silk ties, 3 mm apart, were placed on the left iliac vein, ~1-cm cephalad of the fistula to keep the width of the vein <1.5 mm, after AVF creation or sham operation for 28 days ( $n = 6$  for each). This treatment significantly reduced blood flow, from  $9.8 \pm 1.3$  to  $2.6 \pm 0.7$  mL  $min^{-1}$  measured on the day of fistula construction.

**Chronic delivery of specific inhibitors.** The miniosmotic pumps (model 2004; Alzet, Cupertino, Calif) were prepared as described previously with a modification.<sup>18</sup> After filling the vehicle or drug solution in the pump, a PE-50 tube was connected to flow moderator of pump. The other end of PE tube was then placed into left external jugular vein and the pump was implanted subcutaneously according to the manufacturer's instruction. All procedures were performed under sterile conditions. Vehicle solution (0.05% DMSO) or cell-permeable inhibitors of CaMK II (KN-93, 2.0  $\mu g \mu L^{-1}$ ) or TRPV1 (capsazepine, Capz, 0.2  $\mu g \mu L^{-1}$ ) was carefully filled into pump for 28-day delivery ( $n = 6$  for each test).

**Histologic examination and immunofluorescent staining.** Sections (5  $\mu m$ ) were prepared and stained with hematoxylin and eosin to determine the thickness of the intima and media as described previously.<sup>4</sup> The stained tissue slices were examined using imaging software with a microruler (Spot; Diagnostic Instruments, Sterling Heights, Mich) and the thickness of each layer was measured. The micrographs were obtained from images at 800  $\times$  magnification. For immunofluorescent staining, sections were incubated overnight at 4°C with rabbit antibodies (Santa Cruz Biotechnology, Santa Cruz, Calif) against TRPV1 (1:1,000) or eNOS (1:1,000).<sup>4,19</sup> Staining

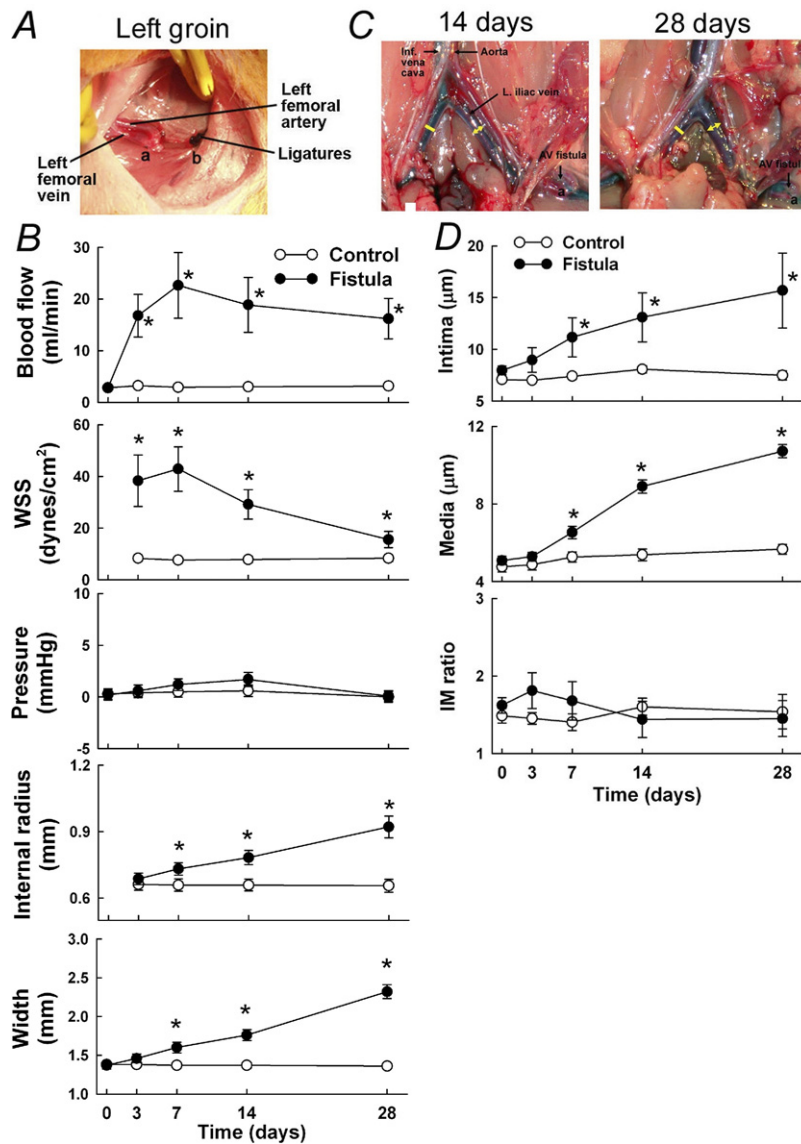


**Fig 1.** Hemodynamic changes and venous remodeling in rat arteriovenous fistula (AVF). **A**, The anastomosis of the femoral artery and vein was created by invagination of the cut end of the artery (b) into the vein (a). **B**, Changes in blood flow, wall shear stress (WSS), intravascular pressure, the internal radius, and width in control and fistula veins at various time points. **C**, Representative images show marked vasodilatation of the iliac vein at the fistula site (indicated by double arrows in yellow) compared with the contralateral site on day 14 and 28. **D**, Changes in the thickness of intima (upper) and media (middle), and the ratio of intima to media (IM) in the veins. \* $P < .05$  compared with control at the same time-point.

with primary antibody preincubated with specific blocking peptides (Santa Cruz Biotechnology) was used as a negative control.

**Reverse transcriptase-polymerase chain reaction analysis (RT-PCR).** Semiquantitative RT-PCR was used to detect TRPV and GAPDH mRNA expression as described previously.<sup>18,19</sup> Briefly, total RNA in the veins was extracted. After the RNA pellet was washed, dried, and resuspended, cDNA was synthesized by using 5  $\mu$ g of the total RNA. TRPV and GAPDH cDNAs were amplified using specific primers

designed as: TRPV1 sense 5'-GCG TTT GTC GAC TGA CTG AA-3' and antisense 5'-CAG GAG TCC AGC TCA CCT TC-3' (transcript product of 396 bases); TRPV4 sense 5'-GTG CCT GGG CCC AAG AAA-3' and antisense 5'-GGG CAG CTC CCC AAA GTA GAA-3' (transcript product of 579 bases); GAPDH sense 5'-TTA GCA CCC CTG GCC AAG G-3' and antisense 5'-CTT ACT CCT TGG AGG CCA TG-3' (transcript product of 535 bases). TRPV mRNA level was expressed as the ratio of the TRPV1 or TRPV4 and GAPDH PCR products.

**Western blot analysis.** Total protein was prepared from venous tissue as described previously.<sup>4,18</sup> Briefly, Western blotting was performed using specific antibodies (Santa Cruz Biotechnology) with appropriate dilution against rat TRPV1 (1:1,000), TRPV4 (1:1,000), eNOS (1:1,500), iNOS (1:1,000), arginase I (1:1,500), arginase II (1:500), phosphorylated CaMK II (pCaMK II; 1:500), total CaMK II (1:500), or actin (1:2,000). After being washed, the membrane was incubated with horseradish peroxidase-conjugated anti-rabbit or anti-mouse IgG antibody (Vector Laboratory, Burlingame, Calif) and bound antibody was visualized using a commercial ECL kit (GE Healthcare Biosciences, Pittsburgh, Pa) and Kodak film. The densities of the bands were determined using an image analyzing system (Diagnostic Instruments).

**Zymography.** MMP2 activity was assayed by gelatin zymography.<sup>20</sup> Gelatin (1 mg ml<sup>-1</sup>) was polymerized in a 10% polyacrylamide gel. Electrophoresis was carried out at 4°C. The gel was washed twice with washing buffer (50 mmol/L Tris-HCl, pH 7.5, 100 mmol/L NaCl, 2.5% Triton X-100), followed by a brief rinse in washing buffer without Triton X-100. Assays were conducted in incubation buffer (50 mmol/L Tris-HCl, pH 7.5, 150 mmol/L NaCl, 10 mmol/L CaCl<sub>2</sub>, 0.02% NaN<sub>3</sub>, and 1 μmol/L ZnCl<sub>2</sub>) at 37°C for 18 hours and visualized by Coomassie Blue R-250 staining. Gelatin digestion appeared as a clear zone.

**Determination of NO metabolites.** Venous samples were prepared according to the manufacturer's instructions and analyzed in duplicate using a commercial kit for nitrate and nitrite (Cayman Chemical, Ann Arbor, Mich).<sup>21</sup>

**Statistics.** Numerical data are presented as the mean ± SEM. Differences between groups were analyzed using an unpaired *t* test or one-way analysis of variance (ANOVA), using Duncan's multiple-range test post-hoc. Significant differences (*P* < .05) are indicated.

## RESULTS

**Remodeling of fistula veins.** After creation of an AVF (Fig 1, A), blood flow in the fistula veins abruptly increased, reaching more than ninefold higher than control veins on day 7 and remained significantly high for 28 days (top panel in Fig 1, B). WSS peaked on day 3 but decreased thereafter, although it was still significantly higher than controls through day 28 (the second panel in Fig 1, B). The increases in blood flow could not be ascribed to altered intravascular pressure, as this parameter remained unchanged at all time-points in both groups (the third panel in Fig 1, B). The internal radius and external width of the iliac vein increased markedly compared with control veins by day 7 and the increase continued thereafter (bottom panel in Fig 1, B). The representative images show venodilatation of the fistula side, compared with the contralateral side, on day 14 and day 28 in AVF rats (Fig 1, C). Despite venodilatation, the thickness of both the intima and media in the fistula veins gradually increased to a level significantly greater than the control group by day 7, and the increases continued thereafter (top and middle panels in Fig 1, D).

However, the intima-to-media (IM) ratio was unchanged (bottom panel in Fig 1, D).

**TRPV expression and hemodynamic changes.** We next examined expression of two TRPV channels during venous remodeling. In the fistula veins, TRPV1 expression increased significantly by day 3 and remained at significantly higher levels thereafter, compared with control veins, with a maximum increase of 5.1-fold on day 7 (Fig 2, A). In contrast, TRPV4 expression was unchanged at all time points. The increases in TRPV1 mRNA expression were similar to the increases in protein level, with peak levels detected on day 7. Again, TRPV4 mRNA expression was unchanged (Fig 2, B). Immunofluorescence labeling revealed that TRPV1 was mostly distributed in the endothelial layer of the control veins and this expression was markedly upregulated in the thickened wall of the 7-day and 14-day fistula veins (Fig 2, C). No signal was detected in the negative control. Linear regression analysis revealed a positive correlation between WSS and TRPV1 protein expression (*R* = 0.7160, Fig 2, D), but there was no correlation to TRPV4 expression (data not shown). Prevention of fistula venodilatation significantly reduces blood flow, WSS, and TRPV1 expression after 28 days (Fig 2, E and F). However, blood flow restriction showed no effect upon control veins.

**CaMK II signaling and NO dysregulation in fistula remodeling.** As a ubiquitous Ca<sup>2+</sup>-dependent enzyme in the vasculature,<sup>22</sup> we examined whether CaMK II activity is correlated with enhanced TRPV1 expression. CaMK II activity calculated by the ratio of phosphorylated to total protein expression was significantly increased at both 14 and 28 days after creation of AVF in the fistula veins compared with control veins (Fig 3, A). This change was associated with a 2.2-fold and 3.1-fold increase in eNOS expression in 14- and 28-day fistula veins, respectively. However, iNOS expression was unchanged (Fig 3, B). eNOS was present in the endothelium and SMCs of the control veins, but its expression was significantly increased in the 14- and 28-day fistula veins, and a major change in protein level was detected in the SMC layer of the fistula veins (Fig 3, C). Interestingly, increased TRPV1 expression in the 28-day fistula vein was colocalized primarily with increased eNOS expression in the endothelial layer.

In addition to the NOS expression, two isoforms of arginase were also present in veins (Fig 3, D) and possibly serve as an endogenous competitor for L-arginine.<sup>23</sup> The expression of arginase I, but not arginase II, was significantly diminished in the 14- and 28-day fistula veins (upper panel). Compared with control veins, arginase activity decreased at both time points in the fistula veins (lower panel). These observations indicate that the changes in arginase activity were due primarily to the downregulation of arginase I.

We further asked whether the increase in CaMK II activity affected the expression of eNOS and arginase I. Treatment of 28-day fistula veins with the specific CaMK II inhibitor KN-93 significantly attenuated eNOS upregulation and restored arginase I expression, compared with

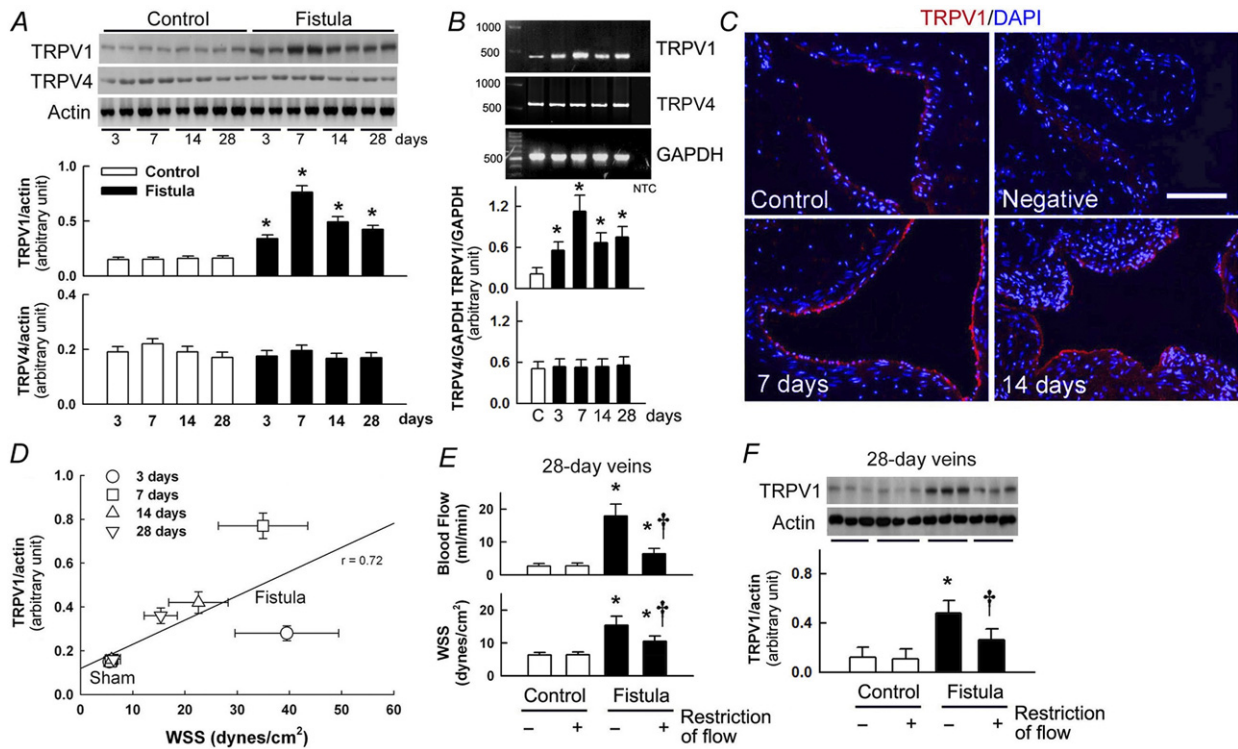


**Fig 2.** Transient receptor potential vanilloid channel (*TRPV*) expression in veins. **A**, Representative blots showing *TRPV1* and *TRPV4* protein levels in the vein ( $n = 2$ ). The bar graphs show a densitometric quantitation of the *TRPV* to actin ratio. **B**, RT-PCR analysis of changes in *TRPV1* and *TRPV4* mRNA in control (C) and fistula veins at various times. **C**, *TRPV1* (red) is present in endothelium of the control and 7- and 14-day fistula veins. Nuclei are stained with DAPI (blue). Scale bar: 100  $\mu\text{m}$ . **D**, Linear regression analysis of wall shear stress (WSS) and *TRPV1* protein levels in veins. **E** and **F**, Vessel restriction by ligature reduces blood flow and WSS (**E**) as well as *TRPV1* protein levels (**F**).  $N = 6$  in all bar graphs. \* $P < .05$  compared with control (at the same time-point in **A**). † $P < .05$  compared with the untreated fistula vein.

untreated veins (Fig 3, E). These results indicate that CaMK II regulates eNOS and arginase I expression reciprocally. Inhibition of CaMK II by KN-93 only slightly reduced *TRPV1* upregulation in the fistula veins ( $P > .05$ , data not shown). The internal diameter and blood flow of fistula veins were also slightly increased by KN-93 treatment. This causes a significant reduction in WSS compared with the untreated fistula veins (data not shown).

An imbalance in arginase I and eNOS activity could cause NO overproduction, and the nitrate and nitrite (NOx) content, representing NO formation, was determined to verify the role of NO in the high WSS vessels. Compared with the control veins, the accumulation of NOx increased significantly in the 14- and 28-day fistula veins, with the highest levels at 28 days (Fig 3, F).

The NO increase was, in fact, a predictor of MMP2 activation in the fistula veins because NO targets zinc ions as well as cysteine residues, which disrupts the cysteine-zinc interaction in MMP and activates the enzyme.<sup>24</sup> Gel zymography demonstrated that the activity of both the proenzyme and the active form of MMP2 significantly increased in 14- and 28-day fistula veins compared with control veins (Fig 3, G).

**Capsazepine attenuates fistula remodeling.** In control veins, neither the external width nor the hemodynamic parameters were affected by treatment with capsazepine or vehicle (Fig 4, A). Capsazepine also showed little effect on intravascular pressure in control or fistula veins (data not shown). However, capsazepine significantly increased the internal radius and slightly increased the blood flow in 28-day fistula veins compared with untreated veins (upper and middle panels). Interestingly, high WSS in the 28-day fistula veins was significantly reduced by capsazepine compared with untreated veins (lower panel).

Capsazepine had no effect on the thickness of the intima and media of the control veins over the 28-day experimental period (upper pictures and lower bar graph of Fig 4, B). However, the drug significantly attenuated vascular remodeling in 28-day fistula veins, as shown by the simultaneous reductions in thickening of the intima and media (lower pictures and bar graph). The ratio of intima-to-media thickness was similar among groups (bottom bar graph).

**Capsazepine reverses downstream signaling for remodeling.** The above observations clearly show that *TRPV1* function is important for venous remodeling. We

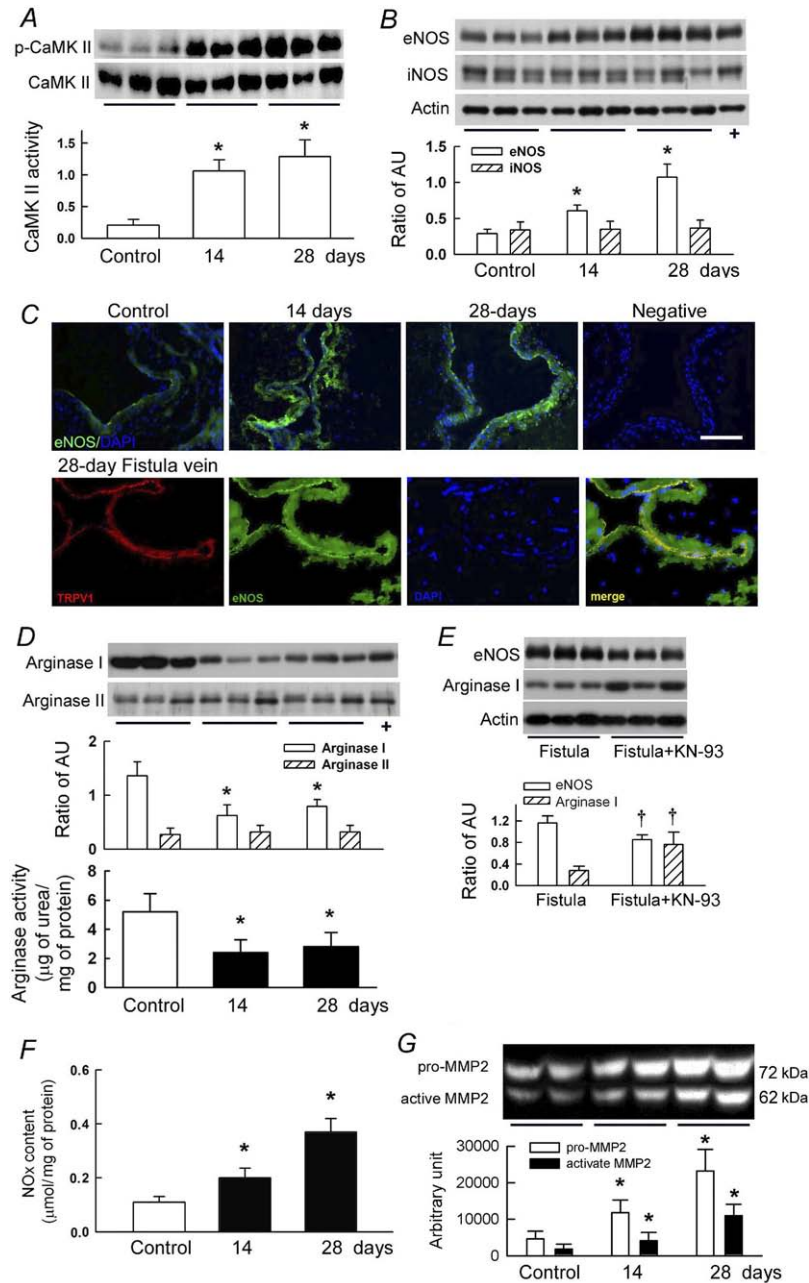


**Fig 3.** Changes in enzymes controlling nitric oxide (NO) production and metalloproteinases (MMP)2 activation in veins. **A**, Western blot shows the expression of phosphorylated and total CaMK II. The bar graph shows the ratio of the two proteins and represents CaMK II activity. **B**, Expression of eNOS and iNOS in veins. AU, Arbitrary units of band density. **C**, Upper panels show that eNOS (green) is present in the veins, and lower panels show the colocalization (yellow in merge picture) of transient receptor potential vanilloid channel 1 (TRPV1) (red) and eNOS (green) in endothelium of a 28-day fistula vein. Nuclei are stained with DAPI (blue). Scale bar: 100 µm. **D**, Expression of arginase I and II in veins. **E**, A specific blocker of CaMK II, KN-93, reverses eNOS and arginase I expression in the 28-day fistula vein. **F**, Content of two NO metabolites, nitrate and nitrite (NOx), in veins. **G**, Zymography reveals that both the proenzyme and active forms of MMP2 have increased activity in the fistula veins. N = 6 in all bar graphs. \*P < .05 compared with the control. †P < .05 compared with the untreated fistula vein.

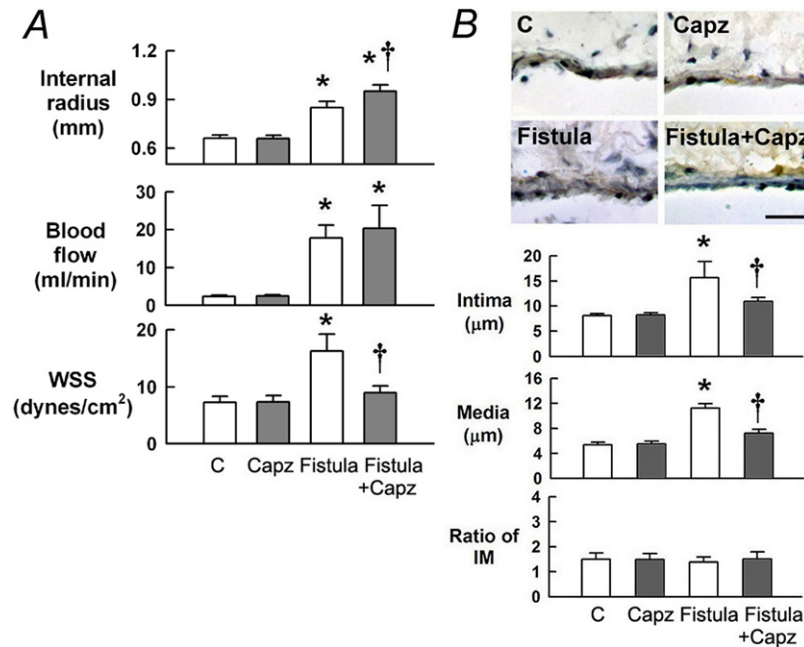


**Fig 4.** Capsazepine attenuates remodeling. **A**, Hemodynamic changes in veins. **B**, Representative images and quantitation of changes in the thickness of intima and media, and the ratio of intima to media (*IM*) in the venous wall. Nuclei are stained by hematoxylin (*blue*). Scale bar: 20  $\mu\text{m}$ .  $N = 6$  in all bar graphs. \* $P < .05$  compared with the control veins (C). † $P < .05$  compared with the untreated fistula vein.

further examined the changes in cellular signaling about the role of TRPV1. Treatment of 28-day fistula veins with capsazepine did not affect the increase in TRPV1 expression (Fig 5, A), whereas the capsazepine treatment significantly reduced CaMK II activation, compared with untreated veins (Fig 5, B). This result suggests that capsazepine possibly blocks  $\text{Ca}^{2+}$  entry through TRPV1, but does not affect its expression. Although CaMK II is a  $\text{Ca}^{2+}$ -dependent enzyme, we cannot rule out the possibility that a different pathway, other than the change in  $[\text{Ca}^{2+}]_i$ , caused by capsazepine may lower CaMK II activity directly. Moreover, the upregulation of eNOS and downregulation of arginase I in the 28-day fistula veins were reversed by capsazepine treatment (Fig 5, C). This change was also correlated with reduced NO formation and MMP2 activity (Fig 5, D and E). NOx formation, MMP2 activity, and protein expression in the control veins were not affected by capsazepine treatment.

## DISCUSSION

We have shown here for the first time that the presence of TRPV1 in the endothelium of the fistula vein is responsive to increased blood flow/WSS in venous remodeling (Fig 6). Endothelial TRPV1 increases CaMK II activity, possibly via  $\text{Ca}^{2+}$  influx, which triggers NO-mediated MMP2 activation by enhancing eNOS and suppressing arginase I expression. Chronic inhibition of TRPV1 lowered CaMK II activity, rebalanced eNOS and arginase I levels, and possibly prevented remodeling.

Various factors can influence vessel remodeling.<sup>25</sup> Wound healing processes, inflammation, and infections also have a profound effect on the vessels in the wound.<sup>26</sup> Our model provides direct evidence that a simple hemodynamic force, ie, high blood flow or WSS, contributes to remodeling of the fistula vein in the absence of any effect caused by surgical wounding. Importantly, several features present in the rat model of femoral AVF are similar to clinically constructed AVF used for hemodialysis. First, the hemodynamic changes, ie, high blood flow and low pressure, resemble those seen in a clinically generated AVF. Second, there was both outward (venodilatation) and inward (shrinkage) remodeling of the vein that correlated well with clinical AVF. Third, the vascular remodeling associated with upregulation of MMPs may account for the changes in the extracellular matrix (ECM) seen in the venous segment of the AVF. However, the present AVF model still has features distinct from the clinically generated AVF. First, the method of AVF creation is not the same as the most frequently used clinical approach of anastomosis, ie, the venous end to arterial side opening technique. Second, the rat iliac veins belong to the deep venous system in contrast to the superficial veins used in uremic patients.

Correction of high blood flow by narrowing the external diameter of the fistula veins not only significantly blocked the flow/WSS increase, but also prevented fistula remodeling over the 28-day experimental period (Fig 2, E and F). These results clearly indicate that high flow/WSS is the primary factor required to cause venous remodeling of

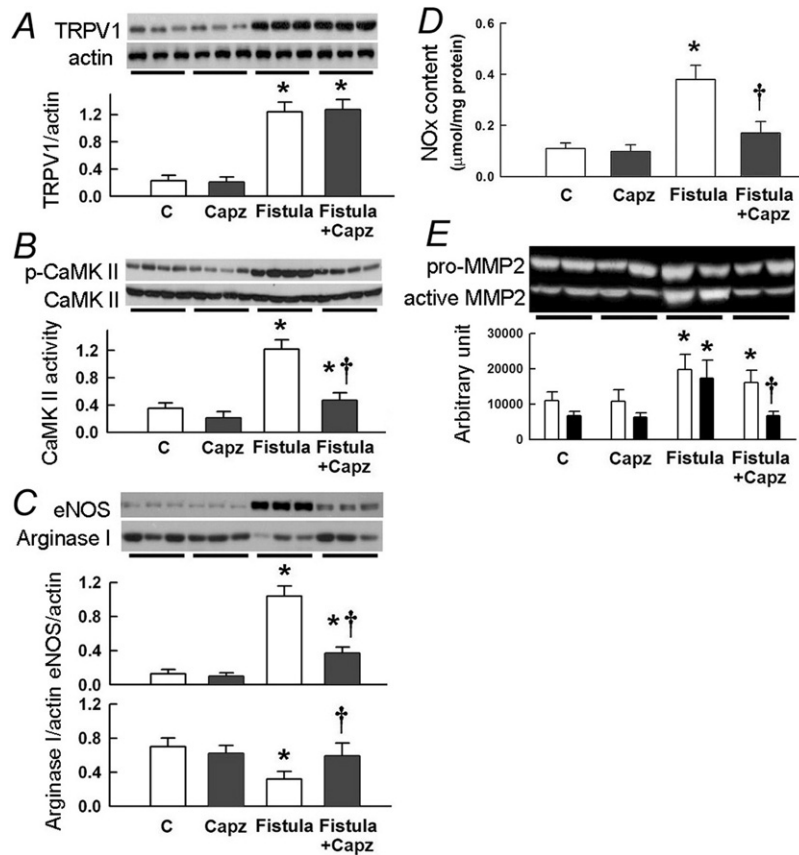


**Fig 5.** Effects of transient receptor potential vanilloid channel 1 (*TRPV1*) blockade. **A** through **C**, Western blots showing *TRPV1* expression, CaMK II activity, or eNOS and arginase I expression in veins in the presence or absence of capsazepine treatment. **D**, Nitric oxide (*NO*) metabolites (*NOx*) in the veins. **E**, Zymography revealing changes in the activity of both the proenzyme and the active form of metalloproteinases (*MMP2*) in the veins. N = 6 in all bar graphs. \**P* < .05 compared to the control veins (C). †*P* < .05 compared with the untreated fistula vein.

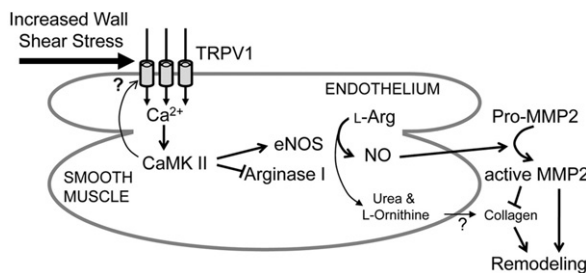


**Fig 6.** Model showing how transient receptor potential vanilloid channel 1 (*TRPV1*) contributes to high blood flow-induced venous remodeling.

AVF and indicates that there must be a sensor present in the veins to detect hemodynamic changes. As a mechanosensitive channel, TRPV channels expressed in various tissues are activated by a broad range of mechanical stimuli.<sup>27,28</sup> Our results are consistent with previous observations, but only *TRPV1* responds to high blood flow in the fistula vein, as *TRPV4* expression was not affected by high flow or

fistula remodeling (Fig 2, A and Fig 5, F). Substantial evidence has emerged indicating that several TRP isoforms may contribute to SMC differentiation during vascular injury.<sup>7</sup> In organ cultures of human saphenous veins, the expression of type 1 canonical TRP (*TRPC1*) was increased in the neointimal growth region of SMCs and application of a *TRPC1*-specific antibody effectively prevented intraluminal narrowing.<sup>29</sup> Oancea et al<sup>30</sup> provided intriguing evidence that in HEK293T cells, exposure to fluid flow rapidly increases the level of the endogenous type 7 melastatin TRP (*TRPM7*) protein in the plasma membrane. A previous study has demonstrated that the functional *TRPV1* channel is a tetramer and that the four subunits interact via the TRP-like domain before trafficking to the plasma membrane.<sup>31</sup> However, this nontranscriptional regulation of *TRPV1* is probably not seen in our fistula veins because we show that both the protein and mRNA levels of *TRPV1* are increased (Fig 2, A and B).

Mechanosensitive channels (MSCs) can be directly activated by force conveyed through lipid tension or structure-linking proteins that respond to the force parallel to the cell



membrane.<sup>32</sup> Ito et al<sup>33</sup> demonstrated that the mechanical stretch applied to human pulmonary microvascular endothelial cells pulled actin-based cytoskeletal stress fibers that in turn, opened TRPV channels. Force also can be detected by a mechanosensitive protein without a channel pore structure which, in turn, triggers production of second messengers that carry the signal to specific TRPV channels for indirect activation.<sup>11,12,32</sup> Elevation of intravascular pressure in rat mesenteric arteries was shown to generate the arachidonate metabolite in SMCs, which subsequently activated TRPV1 for regulation of vascular tone.<sup>11</sup> TRPV4 is present in the endothelium of the rat carotid artery and causes vasodilatation in response to shear stress; this effect is dependent on the action of PLA<sub>2</sub>.<sup>12</sup> These results indicate that an upstream factor is present and acts as the real mechanosensor to induce lipid metabolite generation for TRPV activation. However, whether arachidonate-mediated signal transduction or actin cytoskeleton participated in TRPV1-induced venous remodeling requires detailed studies.

CaMK II in the endothelium is activated by oscillatory or large WSS in vessels with atherosclerotic lesions.<sup>34</sup> Our results also show that the increased CaMK II activity in the fistula veins. This, however, is dependent on TRPV1 because capsazepine markedly attenuated CaMK II activity (Fig 5, B). Because the potential target of increased CaMK II activity is eNOS,<sup>22</sup> the TRPV1-mediated increase in CaMK II activity in our fistula veins may directly stimulate eNOS activity/expression and enhance NO formation during remodeling. Not only an elevation of eNOS expression, but also a reduction in the expression of the endogenous NOS competitor arginase I, is responsible for the increase in NO in the fistula veins (Fig 3, D). Two arginases are present in the endothelium and SMCs of the aorta and coronary artery of various mammalian species.<sup>35</sup> Here, we showed that both arginase I and II were present in the rat iliac vein. However, arginase I is the dominant isoform and contributes to changes in the total arginase activity in the 28-day fistula veins (Fig 3, D). Low arginase expression/activity makes more L-arginine available for eNOS and can also lead to generation of superoxide anions if eNOS becomes "uncoupled". A recent study has reported that an increase in arginase I expression/activity plays an integral role in the remodeling response of rat carotid arteries after injury by balloon inflation.<sup>35</sup> However, we found a sustained downregulation and low activity of arginase I in venous remodeling that was controlled by CaMK II activity (Fig 3). Different vascular tissues and the degree of injury may be the cause of this discrepancy.

A gradual increase in NO formation was seen during fistula remodeling (Fig 3, F). NO or peroxynitrite (ONOO-), which result from simultaneous production of NO and superoxide, activates MMPs.<sup>24</sup> Pro-MMP2 can be activated by removal of the auto-inhibitory propeptide resulting in an active truncated MMP2. In the rabbit AVF, high blood flow in the left common

carotid artery after creating a fistula to the external jugular vein induced NO production, which in turn increased the amount of the 62-kDa active form of MMP2.<sup>36</sup> Our gelatin zymography assay showed similar results in that the activity of both the pro-enzyme and the active MMP2 gradually increased in fistula veins (Fig 3, G). NO and ONOO- can directly react with the cysteine residue in the propeptide domain of MMP2 and disrupt its binding to the catalytic Zn<sup>2+</sup> ion, thereby activating the full-length pro-MMP2.<sup>24</sup> Therefore, increases in both the full-length and active form of MMP2 possibly contribute to ECM remodeling of fistula veins.

In regard to other effects possibly mediated by TRPV1, the previous study has shown that Ca<sup>2+</sup> entry via TRP channels regulate SMC tone by activation of voltage-dependent Ca<sup>2+</sup> channels or enhanced Ca<sup>2+</sup> spark activity of ryanodine receptors and the activity of large-conductance Ca<sup>2+</sup>-sensitive K<sup>+</sup> channels.<sup>37</sup> Moreover, TRPV1 can be phosphorylated by several kinases including CaMK II, the dynamic balance between the rate of phosphorylation and dephosphorylation controls TRPV1 activity.<sup>31</sup> Together with unchanged TRPV1 upregulation in the KN-93-treated fistula veins, we speculate that increased CaMK II activity in the fistula veins only affect channel activity but not protein level of TRPV1. Membrane stretch activates several Gq-coupled receptors,<sup>38</sup> which then increase phospholipase C (PLC) activity, in a large array of cells and tissues.<sup>39</sup> PLC elevates cellular levels of PIP<sub>2</sub>, DAG, and IP<sub>3</sub>, all of which have been demonstrated to influence TRP channel activity. Interestingly, protein kinase C-dependent phosphorylation of TRPV1 occurs downstream of activation of Gq-coupled receptors.<sup>31</sup> However, which of the above mechanisms is involved in enhanced TRPV1 function in the fistula veins requires further study.

Though the venous segment of the AVF produces a vasodilator response to reduce WSS, the persistent presence of high blood flow causes wall thickening in the fistula veins and creates more tensile stress than found in control veins as a result of the high WSS (Fig 1, B), which eventually results in exaggerated remodeling. We restricted the high blood flow in fistula veins and showed that this treatment attenuates WSS and TRPV1 upregulation (Fig 2, E and F). This indicates that physical factors is primarily responsible for wall thickening. However, flow restriction is not practical in clinical settings because high flow is required for blood delivery during dialysis. Interestingly, TRPV1 inhibition markedly reduced WSS-induced remodeling and did not affect other hemodynamic changes such as high blood flow (Fig 4). Moreover, capsazepine treatment showed little effect on the increased level of pro-MMP2 in the fistula veins (Fig 5, E). This indicates that the fistula veins still accumulate pro-remodeling molecules, but components such as TRPV1, which initiate remodeling, are blocked. We therefore speculate that blockade of TRPV1 function may delay or optimize venous remodeling during maturation.

## CONCLUSION

Our results indicate that TRPV1 is essential in the remodeling of fistula veins, and that WSS leads to TRPV1 upregulation. Blockade of the sensor function of TRPV1 prevents venous thickening and makes fistula veins more distensible when challenged with a similar high flow.

## AUTHOR CONTRIBUTIONS

Conception and design: Y-SC, M-JL, H-SH, M-CM

Analysis and interpretation: Y-SC, M-JL, M-CM

Data collection: M-JL, M-CM

Writing the article: M-CM

Critical revision of the article: Y-SC, M-CM

Final approval of the article: Y-SC, M-JL, H-SH, M-CM

Statistical analysis: Y-SC, M-JL, M-CM

Obtained funding: Y-SC, M-JL, H-SH, M-CM

Overall responsibility: Y-SC, M-CM

Y-SC and M-JL contributed equally to this study.

## REFERENCES

- Konner K, Nonnast-Daniel B, Ritz E. The arteriovenous fistula. *J Am Soc Nephrol* 2003;14:1669-80.
- Corpataux JM, Haesler E, Silacci P, Ris HB, Hayoz D. Low-pressure environment and remodelling of the forearm vein in Brescia-Cimino haemodialysis access. *Nephrol Dial Transplant* 2002;17:1057-62.
- Asif A, Roy-Chaudhury P, Beathard GA. Early arteriovenous fistula failure: a logical proposal for when and how to intervene. *Clin J Am Soc Nephrol* 2006;1:332-9.
- Chan CY, Chen YS, Ma MC, Chen CF. Remodeling of experimental arteriovenous fistula with increased matrix metalloproteinase expression in rats. *J Vasc Surg* 2007;45:804-11.
- Owens GK, Kumar MS, Wamhoff BR. Molecular regulation of vascular smooth muscle cell differentiation in development and disease. *Physiol Rev* 2004;84:767-801.
- Brakemeier S, Eichler I, Hopp H, Köhler R, Hoyer J. Up-regulation of endothelial stretch-activated cation channels by fluid shear stress. *Cardiovasc Res* 2002;53:209-18.
- Inoue R, Jensen LJ, Shi J, Morita H, Nishida M, Honda A, et al. Transient receptor potential channels in cardiovascular function and disease. *Circ Res* 2006;99:119-31.
- Miller VM, Barber DA. Modulation of endothelium-derived nitric oxide in canine femoral veins. *Am J Physiol* 1996;271:H668-73.
- Lam CF, Peterson TE, Richardson DM, Croatt AJ, d'Uscio LV, Nath KA, et al. Increased blood flow causes coordinated upregulation of arterial eNOS and biosynthesis of tetrahydrobiopterin. *Am J Physiol Heart Circ Physiol* 2006;290:H786-93.
- Tuttle JL, Nachreiner RD, Bhuller AS, Condict KW, Connors BA, Herring BP, et al. Shear level influences resistance artery remodeling: wall dimensions, cell density, and eNOS expression. *Am J Physiol Heart Circ Physiol* 2001;28:H1380-9.
- Scotland RS, Chauhan S, Davis C, De Felipe C, Hunt S, Kabir J, et al. Vanilloid receptor TRPV1, sensory C-fibers, and vascular autoregulation: a novel mechanism involved in myogenic constriction. *Circ Res* 2004;95:1027-34.
- Köhler R, Heyken WT, Heinau P, Schubert R, Si H, Kacik M, et al. Evidence for a functional role of endothelial transient receptor potential V4 in shear stress-induced vasodilatation. *Arterioscler Thromb Vasc Biol* 2006;26:1495-502.
- Birder LA, Nakamura Y, Kiss Nealen ML S, Barrick S, Kanai AJ, et al. Altered urinary bladder function in mice lacking the vanilloid receptor TRPV1. *Nat Neurosci* 2002;5:856-60.
- Zhang H, Liu YX, Wu YM, Wang ZM, He RR. Capsaicin facilitates carotid sinus baroreceptor activity in anesthetized rats. *Acta Pharmacol Sin* 2004;25:1439-43.
- Feng NH, Lee HH, Shiang JC, Ma MC. Transient receptor potential vanilloid type 1 channels act as mechanoreceptors and cause substance P release and sensory activation in rat kidneys. *Am J Physiol Renal Physiol* 2008;294:F316-25.
- Dumont O, Loufrani L, Henrion D. Key role of the NO-pathway and matrix metalloproteinase-9 in high blood flow-induced remodeling of rat resistance arteries. *Arterioscler Thromb Vasc Biol* 2007;27:317-24.
- Castier Y, Brandes RP, Leseche G, Tedgui A, Lohou S. p47phox-dependent NADPH oxidase regulates flow-induced vascular remodeling. *Circ Res* 2005;97:533-40.
- Lin JS, Chen YS, Chiang HS, Ma MC. Hypoxic preconditioning protects rat hearts against ischemia/reperfusion injury: role of erythropoietin on progenitor cell mobilization. *J Physiol* 2008;586:5757-70.
- Bratz IN, Dick GM, Tune JD, Edwards JM, Neeb ZP, Dincer UD, et al. Impaired capsaicin-induced relaxation of coronary arteries in a porcine model of the metabolic syndrome. *Am J Physiol Heart Circ Physiol* 2008;294:H2489-96.
- Kim KH, Cho YS, Park JM, Yoon SO, Kim KW, Chung AS. Pro-MMP-2 activation by the PPARgamma agonist, ciglitazone, induces cell invasion through the generation of ROS and the activation of ERK. *FEBS Lett* 2007;581:3303-10.
- Huang HS, Ma MC, Chen J. Chronic L-arginine administration increases oxidative and nitrosative stress in rat hyperoxaluric kidneys and excessive crystal deposition. *Am J Physiol Renal Physiol* 2008;295:F388-96.
- Schneider JC, El Kebir D, Chéreau C, Lanone S, Huang XL, De Buys Roessingh AS, et al. Involvement of Ca2+/calmodulin-dependent protein kinase II in endothelial NO production and endothelium-dependent relaxation. *Am J Physiol Heart Circ Physiol* 2003;284:H2311-9.
- Durante W, Johnson FK, Johnson RA. Arginase: a critical regulator of nitric oxide synthesis and vascular function. *Clin Exp Pharmacol Physiol* 2007;34:906-11.
- Chow AK, Cena J, Schulz R. Acute actions and novel targets of matrix metalloproteinases in the heart and vasculature. *Br J Pharmacol* 2007;152:189-205.
- Pasterkamp G, Galis ZS, de Kleijn DP. Expansive arterial remodeling: location, location, location. *Arterioscler Thromb Vasc Biol* 2004;24:650-7.
- Wong V, Ward R, Tayler J, Selvakumar S, How TV, Bakran A. Factors associated with early failure of arteriovenous fistulae for haemodialysis access. *Eur J Vasc Endovasc Surg* 1996;12:207-13.
- O'Neil RG, Heller S. The mechanosensitive nature of TRPV channels. *Pflugers Arch* 2005;451:193-203.
- Ciura S, Bourque CW. Transient receptor potential vanilloid 1 is required for intrinsic osmoreception in organum vasculosum lamina terminalis neurons and for normal thirst responses to systemic hyperosmolality. *J Neurosci* 2006;26:9069-75.
- Kumar B, Dreja K, Shah SS, Cheong A, Xu SZ, Sukumar P, et al. Upregulated TRPC1 channel in vascular injury in vivo and its role in human neointimal hyperplasia. *Circ Res* 2006;98:557-63.
- Oancea E, Wolfe JT, Clapham DE. Functional TRPM7 channels accumulate at the plasma membrane in response to fluid flow. *Circ Res* 2006;98:245-53.
- García-Sanz G, Fan R, Shah V, Sorrentino R, Cirino G, Papapetropoulos A, et al. Dynamic activation of endothelial nitric oxide synthase by Hsp90. *Nature* 1998;392:821-4.
- Lin SY, Corey DP. TRP channels in mechanosensation. *Curr Opin Neurobiol* 2005;15:350-7.
- Ito S, Suki B, Kume H, Numaguchi Y, Ishii M, Iwaki M, et al. Actin Cytoskeleton regulates stretch-activated Ca2+ influx in human pulmonary microvascular endothelial cells. *Am J Respir Cell Mol Biol* 2009 (in press).
- Cai H, Liu D, Garcia JG. CaM Kinase II-dependent pathophysiological signalling in endothelial cells. *Cardiovasc Res* 2008;77:30-4.

35. Peyton KJ, Ensenat D, Azam MA, Keswani AN, Kannan S, Liu XM, et al. Arginase promotes neointima formation in rat injured carotid arteries. *Arterioscler Thromb Vasc Biol* 2009;29:488-94.
36. Tronc F, Mallat Z, Lehoux S, Wassef M, Esposito B, Tedgui A. Role of matrix metalloproteinases in blood flow-induced arterial enlargement: interaction with NO. *Arterioscler Thromb Vasc Biol* 2000;20:E120-6.
37. Brayden JE, Earley S, Nelson MT, Reading S. Transient receptor potential (TRP) channels, vascular tone and autoregulation of cerebral blood flow. *Clin Exp Pharmacol Physiol* 2008;35:1116-20.
38. Tzima E, Irani-Tehrani M, Kiosses WB, Dejana E, Schultz DA, Engelhardt B, et al. A mechanosensory complex that mediates the endothelial cell response to fluid shear stress. *Nature* 2005;437:426-31.
39. Voets T, Nilius B. TRPCs, GPCRs and the Bayliss effect. *The EMBO Journal* 2009;28:4-5.

Submitted Mar 6, 2010; accepted May 22, 2010.

#### CME Credit Now Available to JVS Readers

Readers can now obtain CME credits by reading selected articles and correctly answering multiple choice questions on the Journal website ([www.jvascsurg.org](http://www.jvascsurg.org)). Four articles are identified in the Table of Contents of each issue and 2 questions for each are posted on the website. After correctly answering the 8 questions, readers will be awarded 2 hours of Category I CME credit.